MODELLING OF ATMOSPHERIC TURBULENCE IN INHOUSE ROTORCRAFT SIMULATION TOOL: CHARACTERIZATION AND COMPARISON

Cenk Çetin, cenk.cetin@tai.com.tr, Turkish Aerospace, Ankara-Turkey

Arda Çalışkan, arda.caliskan@tai.com.tr, Turkish Aerospace, Ankara-Turkey

Kaan Sansal, kaan.sansal@tai.com.tr, Turkish Aerospace, Ankara-Turkey

Volkan Kargın, vkargin@tai.com.tr, Turkish Aerospace, Ankara-Turkey

Abstract

In the present work, integration of an atmospheric turbulence model approximating the von Kármán spectra into the TA Originated Rotorcraft Simulation (TOROS) tool is presented. The integrated atmospheric turbulence content consists of 3D velocity components based on the second order statistics. Prior to the implementation, the model is analyzed in detail. Turbulence model is compared with flight test data along with the helicopter flight dynamics model where the initial trim points and power spectral densities of the helicopter rates are used as validation parameters. The results indicate that injection of the atmospheric turbulence component significantly alter the helicopter control rates representing meaningful agreement with flight test data. In addition, the effect of the different aerodynamic surfaces is also analyzed. The results indicate that turbulence in main rotor is the major contributor to the energy spectrum for the heave and roll rates.

NOMENCLATURE

$E(\Omega)$	:	Energy spectrum.
$L_{u,v,w}$	:	Turbulence length scale, [m].
$\sigma_{u,v,w}$	:	Turbulence intensity, [m/s].
Ω	:	Spatial frequency vector, [rad/m].
ω, ν, κ	:	Spatial frequency components in Cartesian coordinate axes, [rad/m].
S_{uu}, S_{vv}, S_{ww}	:	Power spectral densities in all axis, [m^2/s^2].
u, v, w	:	Turbulent velocity components in atmospheric frame, [m/s].
X, Y	:	Atmospheric frame coordinates, [m].
p, q, r	:	Helicopter angular rates, [deg/s].
ϕ, θ, ψ	:	Helicopter Euler angles, [deg].
δ_{coll}	:	Collective input, [%].
δ_{lon}	:	Longitudinal cyclic input, [%].
δ_{lat}	:	Lateral cyclic input, [%].
δ_{pedal}	:	Pedal input, [%].
t	:	Time, [s].
N_i	:	Spatial instant grid size.
Φ_j	:	White noise input, [rad].

1. INTRODUCTION

Rotorcrafts are designed to perform various complex tasks in their operational envelopes where they often encounter turbulence due to reasons including atmospheric boundary layer, airwake shed from ship or large buildings and atmospheric variations. Presence and severity of turbulence may significantly affect the task performance, handling quality, pilot workload and safety. Considering the aforementioned issues, modelling of turbulence for rotorcraft flight dynamic analysis and simulators becomes significant. The traditional techniques including Dryden and von Kármán model relies on utilization of frozen field approach [1–2] that is a function of flight speed and mostly used for fixed wing applications. These models are well suited for real-time applications due to their computational efficiency and widely used in engineering simulators. However, since they are mostly sampled at aircrafts center of gravity and components are generated in repetitive manner, they received unsatisfactory comments by the pilots. In addition, rotational sampling concept also makes the turbulence modelling in rotorcrafts challenging. Different approaches including, stochastic and empirical modelling [3–8], control equivalent turbulence input modelling [9–11] have been widely implemented to rotorcraft applications within the last 30 years.

In the current work, implementation of the atmospheric turbulence model utilizing the second order statistics of von Kármán spectra is presented. The integration is applied to the in-house simulation tool (TOROS). Comparison with flight test data is discussed. In addition, contributions of different aerodynamic injection locations are investigated. Outcomes for the future work map is addressed.

2. HELICOPTER MODEL

In the present study flight mechanics analysis are performed using TA Originated Rotorcraft Simulation (TOROS), the in-house rotorcraft simulation tool. The tool is built in MATLAB-Simulink® environment. In addition, this tool also supports, handling quality analysis, automatic flight control system design and

real-time flight simulation. Each rotorcraft system is modelled separately in a modular structure and integrated as whole. The validity of the tool is compared and validated against models constructed in commercially available FLIGHTLAB® software in previous studies [12–14]. Fig. 1 represents the trim analysis for low-speed level flight task along with the flight test results of T625 GÖKBEY (Turkish Light Utility Helicopter) during phase 1 development campaign. Low speed test points are performed at 2800 feet pressure altitude with a 5600 kg gross weight aft C.G. configuration whereas high speed cases are performed at 5000 feet pressure altitude with similar configurations. Considering the policy followed during the development phase, limited number of trim points are presented keeping the results blind. It is observed that there is a significant agreement between analysis and flight test results. The discrepancies in collective and longitudinal cyclic controls can be attributed to the difficulty of modelling at low speeds or so-called transition regime due to complex airflow and slight differences in fuselage drag at high angle of attack.

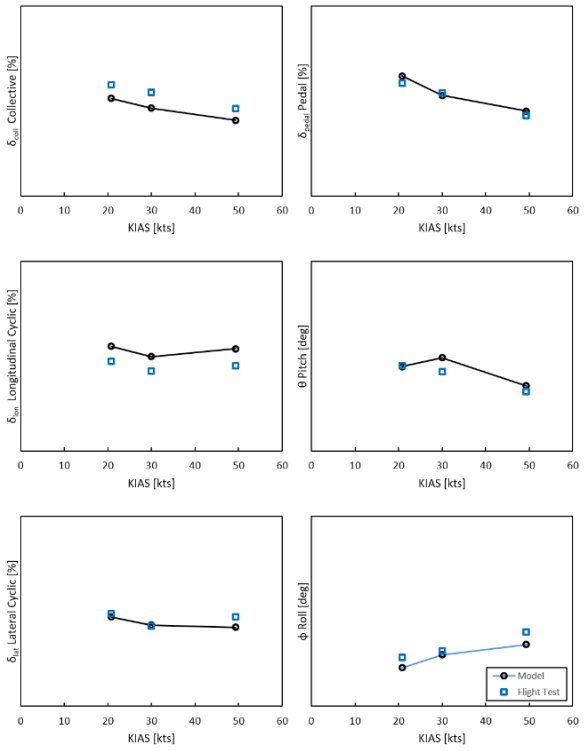

Fig. 1 Trim Analysis and Flight Test Results.

3. ATMOSPHERIC TURBULENCE MODEL

3.1. Generation Scheme

In the present work, atmospheric turbulence content is generated using white noise driven von Kármán filters for which the simple scheme is presented in Fig. 2. This model is based on Taylor's Frozen Field Hypothesis [15] stating that at close neighborhood of a point fixed in atmospheric frame, temporal changes in velocity field are comparably smaller than as of spatial variation. In addition, turbulence field generation relies on assumptions including homogeneity, isotropy, and Gaussian distribution. The current method simulates the turbulence velocity component in three directions varying with spatial position in atmospheric frame.

Fig. 2 Turbulence Generation Scheme.

The energy spectrum of the von Kármán Turbulence model is defined [3] as in the following equation (1):

$$E(\Omega) = \frac{55}{9\pi}\sigma^2 L \frac{(aL\Omega)^4}{[1+(aL\Omega)^2]^{17/6}} \quad (1)$$

in which $\Omega = \omega\, i + \nu\, j + \kappa\, k$ are spatial frequency vector (in [rad/m]), σ is the turbulence intensity (in [m/s]), L is the turbulence length scale and a is the constant ≈ 1.339. For the numerical simulation, a spatial turbulence domain is generated representing the variations in two dimensions longitudinal and lateral axes in terms of spatial frequencies. As Robinson III [6] explained in detail, the rotorcrafts perform tasks at low and moderate altitudes therefore both longitudinal and lateral variations of turbulence field should be considered which makes one dimensional engineering simulation approach unacceptable. In addition, neglecting the variations in normal direction appear as an acceptable practice considering the maximum height difference across the aerodynamic injection locations during the severe maneuvers. Therefore N_1 x N_2 spatial frequency domain is generated for which the Von Kármán energy spectrum reduces to following two dimensional autospectral density functions obtained by double integration represented in the equations (2–4) [3]:

$$S_{uu}(\omega,\nu) = \frac{\sigma_u^2}{6\pi}(aL_u)^2 \frac{1+(aL_u)^2+\left(\omega^2+\frac{11}{3}\nu^2\right)}{[1+(aL_u)^2(\omega^2+\nu^2)]^{7/3}} \quad (2)$$

$$S_{vv}(\omega,\nu) = \frac{\sigma_v^2}{6\pi}(aL_v)^2 \frac{1+(aL_v)^2+\left(\frac{11}{3}\omega^2+\nu^2\right)}{[1+(aL_v)^2(\omega^2+\nu^2)]^{7/3}} \quad (3)$$

$$S_{ww}(\omega,\nu) = \frac{4\sigma_w^2}{9\pi}(aL_w)^4 \frac{(\omega^2+\nu^2)}{[1+(aL_w)^2(\omega^2+\nu^2)]^{7/3}} \quad (4)$$

Turbulence intensity and length scale parameters are found using the military specification MIL-F-8785C and MIL-HDBK-1797 [2] defining the scales according to altitude model. Once the white noise series (Φ_j) is generated for whole grid domain, autospectral densities can be transformed to the time domain using inverse discrete Fourier transform in

order to obtain the turbulence component. This process can be achieved using random process simulation algorithm proposed by Shinozuka [16] applying the summation of sinusoids as function of evenly distributed frequency and random phase over spectral distribution. In the current work, Shinozuka's algorithm is updated benefitting the Borgman's simulation technique [17].

(5)

$$u(X,Y,t) = 2\sqrt{2}\sum_{j=1}^{N_1*N_2}\sqrt{S_{uu}(\omega,\nu)\Delta\omega\Delta\nu}\sin(X\omega_j + Y\nu_j + \Phi_j)$$

(6)

$$v(X,Y,t) = 2\sqrt{2}\sum_{j=1}^{N_1*N_2}\sqrt{S_{vv}(\omega,\nu)\Delta\omega\Delta\nu}\sin(X\omega_j + Y\nu_j + \Phi_j)$$

(7)

$$w(X,Y,t) = 2\sqrt{2}\sum_{j=1}^{N_1*N_2}\sqrt{S_{ww}(\omega,\nu)\Delta\omega\Delta\nu}\sin(X\omega_j + Y\nu_j + \Phi_j)$$

In the current work, turbulence field is generated in each simulation time step at 11 aerodynamic injection points. These points include fuselage, main rotor hub, five main rotor blades (at 0.75R), tail rotor, left and right horizontal stabilizers, and vertical tail. Aerodynamic injection points are illustrated in the following Fig. 3.

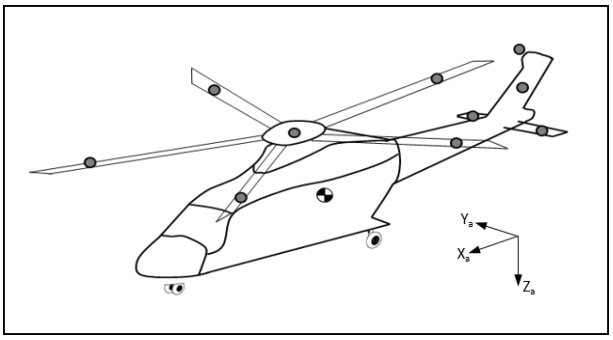

Fig. 3 Turbulence content injection points.

3.2. Sample Simulation Test

The functionality of the aforementioned algorithm is checked for sample cases. Sample simulations are performed for a N_1=80 x N_2=80 rectangular grid for each spatial point. For comparison purposes 120 x 120 domain is also represented. The temporal sampling frequency is set as 30 Hz. The following Fig. 4 shows turbulent velocity component domain in vertical direction along with the comparison of the PSD with theoretical von Kármán spectra and Dryden spectra. The simulated model exhibits an asymptotic distribution with power of -1.72. The slight deviation from -5/3 (~-1.67) power can be attributed to utilization of the white noise as discussed in previous works [6]. The simulated model represents the 2-decade amplitude. Since in the current work implementation and characterization are aimed, the fidelity of the simulation along with the real time application will be proposed as a future work.

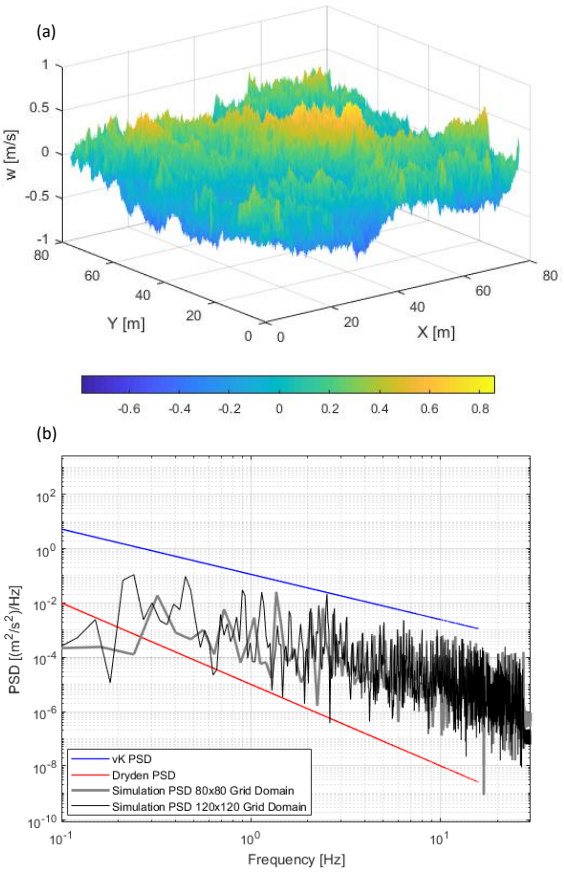

Fig. 4 (a) Sample Turbulence Field, (b) PSD of a Vertical Turbulence Component.

4. RESULTS AND DISCUSSION

4.1. Simulation and Flight Test Comparison at Low Speed

Using the helicopter model introduced in chapter 2, simulations are performed with coupled turbulence model and their results are compared with the trim tasks performed during flight test campaign. The sampling frequency of the flight dynamics simulation model is f_s = 400 Hz satisfying the Nyquist criteria for the turbulence sampling rate thus allowing desired frequency band. Power spectral density (PSD) analysis is applied to the helicopter rates for both simulation and flight-test results. The following Fig. 5 compares the non-dimensional PSDs of helicopter response to the atmospheric turbulence for the third level flight trim task performed at 50 knots and 2800 feet pressure altitude with 4 - 5 knots of mean wind speed. The turbulence intensity is estimated as light at order of 1 – 1.5 knots. Considering the similar approach as in trim results the frequency axis is kept blind. The PSD distributions for flight test results are presented applying the curve fitting. When the decay

rates of the helicopter responses are investigated, simulation results are found in good agreement with flight test results. Similar observation is valid for the PSD magnitudes of the roll, pitch, and yaw rates. However, when heave rate is considered, although decay rates of the model and flight test data are similar, there is a discrepancy between their magnitudes (~15 dB). This can be attributed to the slight difference in collective position estimation. A significant improvement in terms of magnitude and decay rate is obtained compared to the case for which the turbulence model is not coupled.

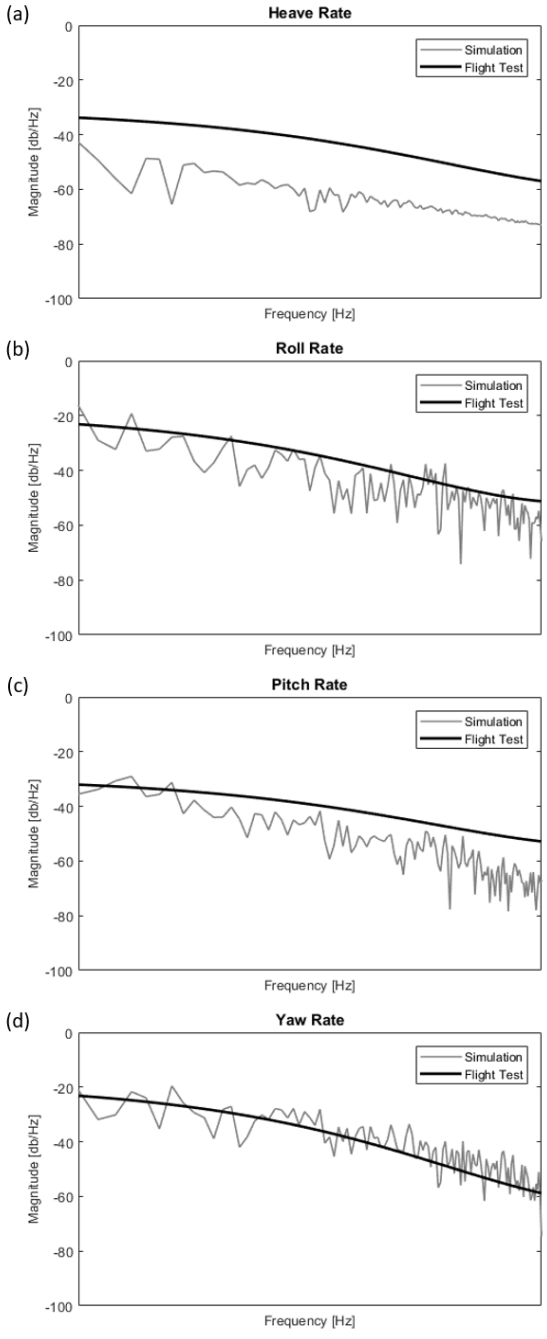

Fig. 5 Helicopter Rates' PSD Comparison: Simulation and Flight Test.

4.2. Simulation and Flight Test Comparison at High Speed

As per the flight test campaign advances, the possibility of higher speed model – test comparison has been arisen. Despite compared flight tests were not performed particularly for turbulence model tuning, it is still believed that such approach will be helpful in terms of planning the future turbulence model development flights. For that purpose, a comparison domain is presented in terms of airspeed. At that period of the campaign the flight data acquired by second prototype so called P2 are used. The P2 is equipped with an air data boom positioned at the nose of the air vehicle where the orientation is as possible as towards forward to be affected at minimum from the MR downwash. The air data boom system is capable of measuring attack angle, sideslip and air speed at high sampling rates and is being used for the calibration of the pitot static system. The air speed is obtained via swivel pressure probe such that free to rotate at a certain envelope orienting itself directly through the wind.

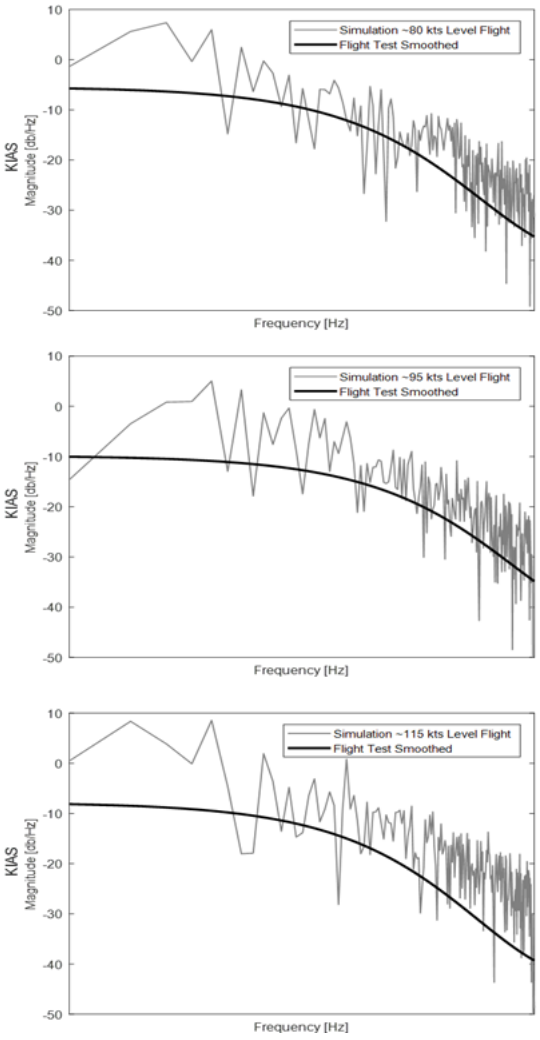

Fig. 6 Helicopter Rates' PSD Comparison: Simulation and Flight Test.

The Fig.6 represents the PSD distribution obtained from the air speed measurement during the level flight tests for 80 to 115 knots indicated air speed. The test points are selected such that, the crew reported the experience of low to medium turbulence during the test where they were allowed to supply hands – on corrective control input along the trimmed flight condition. The test elevation was around 5000 ft pressure altitude. The PSD distributions for flight test results are presented applying the curve fitting for high speed as well. When the decay characteristics of the airspeed for test and simulation is compared, a good agreement in terms of the rate thus the trend is observed at a broadband frequency range.

4.3. Turbulence Injection Point Comparison

The contributions of turbulent velocity injection points that are illustrated in Fig.3 are investigated for simulation case shown in Fig. Contributions of airframe, main rotor, empennage, and tail rotor are represented separately and compared with all points' injection.

The Fig.7 is constructed in same manner with Fig.5. The fourth order fit is applied to all PSDs for the ease of comparison. For heave and roll rates, main rotor appeared as the major contributor to the overall PSDs. This observation is in line with the findings of Ji et al. [7]. For the pitch rate, despite a clear distinction is not apparent among the points at low frequencies, contribution of empennage resembles the overall distribution most. It is widely known that the aft C.G. configuration is among the challenging flight conditions around the transition case where unstable dynamic modes are mostly across the longitudinal channel. Therefore, the injection of turbulence might excite the unstable condition resulting in semi divergence behavior regardless the location. When yaw rate is considered, a clear distinction is not apparent, however empennage dominates the distribution. An explanatory discussion can be supplied by the inclusion of further analysis.

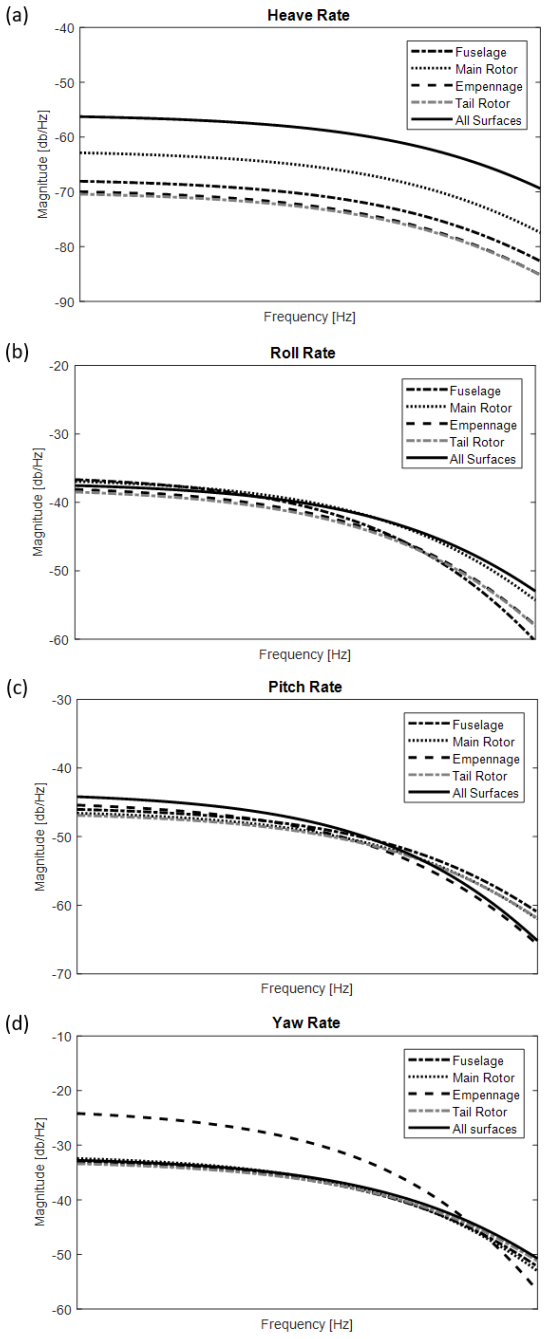

Fig. 7 Simulation PSD comparison: turbulence injection points.

5. CONCLUSION

Implementation of the atmospheric turbulence model based on second order von Kármán spectra is presented. The model is integrated to non-linear flight mechanics model and simulation results are compared with flight test data. Based on the

aforementioned discussions following conclusions can be listed:

1) Theoretical Kolmogorov scale of -5/3th power can be captured by using the implemented model.
2) Angular rates of the real flight results are closely estimated by the injection of turbulence velocity components.
3) Despite a clear difference cannot be assessed, main rotor appears to be major contributor to the heave and roll rate PSDs whereas pitch rate is sensitive to empennage and yaw rate is sensitive to empennage and tail rotor.
4) At higher speeds the energy decay in directed air speed measurements can be approximated, where the improvements and tuning can be performed with particularly designed flight test campaigns.

To conclude, results confirm that for turbulence modelling, second order statistics are satisfactory to estimate realistic helicopter responses in terms of decay rate and magnitude for angular rates and airspeed.

5.1. Current Status

Up to that point, we have built and coupled the following models in TOROS for the turbulence modelling task in our road map:

- von Kármán 1D spectral model [2],
- Control equivalent turbulence injection model (CETI) [10-11], and,
- Presented von Kármán 2D spectral model.

The real time capabilities are also achieved for vK 1D spectral model and CETI model. Further studies are planned to be conducted for implementing current model to in real time working simulator using modified Borgmans method [6], recursive and table look-up methods. Fidelity of the model will also be improved by employing modifications in transfer functions to adjust the harmonics. In addition, CETI model will also be tuned based on a flight test campaign. The progress of aforementioned future work will be the topic of following presentations.

REFERENCES

[1] Etkin, B., “Turbulent wind and its effect on flight,” *Journal of Aircraft*, Vol. 18, (5), 1981, pp. 327-345.

[2] “Flying Qualities of Piloted Airplanes,” U.S. Department of Defense, MIL-SPEC MIL-F-8785C, Washington, D.C., Nov. 1980.

[3] Gaonkar, G. H., “Review of Turbulence Modeling and Related Applications to Some Problems of Helicopter Flight Dynamics,” *Journal of the American Helicopter Society*, Vol. 53, (1), 2008, pp. 87–107.

[4] Elliott, A. S., and Chopra, I., “Helicopter Response to Atmospheric Turbulence in Forward Flight,” *Journal of the American Helicopter Society*, Vol. 35, (2), 1990, pp. 51–59.

[5] Riaz, J., “A Simulation Model of Atmospheric Turbulence for Rotorcraft Applications,” Ph.D. Dissertation, Georgia Institute of Technology, Atlanta, United States, 1992.

[6] Robinson III, J. E., “Real-Time Simulation of Full-Field Atmospheric Turbulence for a Piloted Rotorcraft Simulator,” M.Sc. Dissertation, Massachusetts Institute of Technology, Cambridge, United States, 1994.

[7] Ji, H. L., Chen, R. L., and Li, P., “A Distributed Atmospheric Turbulence Model for Helicopter Flight Simulation and Handling Quality Analysis,” *Journal of Aircraft*, Vol. 54, (1), 2017, pp. 190–198.

[8] Ji, H. L., Chen, R. L., and Li, P., “Analysis of Helicopter Handling Quality in Turbulence with Recursive Von Kármán Model,” *Journal of Aircraft*, Vol. 54, (5), 2017, pp. 1631–1639.

[9] Labows, S., Blanken, C. L., and Tischler, M. B., “UH-60 Black Hawk Disturbance Rejection Study for Hover/Low Speed Handling Qualities Criteria and Turbulence Modeling,” *Proceedings of the 56th Annual Forum of American Helicopter Society*, AHS International, Virginia, May 2000.

[10] Lusardi, J., Tischler, M. B., Blanken, C., and Labows, S. “Empirically derived helicopter response model and control system requirements for flight in turbulence,” *Journal of the American Helicopter Society*, Vol. 49, (3), 2004, pp. 340 - 349.

[11] Seher-Weiss, S., and Von Gruenhagen, W., “Development of EC 135 Turbulence Models via System Identification,” Aerospace Science and Technology, Vol. 23, (1), 2012, pp. 43–52.

[12] K., Sansal, V., Kargin And U., Zengin, "A Generic Ground Dynamics Model For Slope Landing Analysis," *In 72nd Annual Forum Of The American Helicopter Society*, West Palm Beach, Florida, May 17-19, 2016.

[13] K., Şansal, G., Koçak and V., Kargın, "Multi-objective Horizontal Stabilizer Optimization Using Genetic Algorithm," in AHS International 74th Annual Forum & Technology Display, Phoenix, Arizona, May 14-17, 2018.

[14] G., Koçak, K., Şansal, S. Sağıroğlu and V. Kargın, "A Generic Ground Dynamics Model For Ground Handling Evaluations," *in 44th European Rotorcraft Forum*, Delft, the Netherlands, Sep 19-20, 2018.

[15] Taylor G.I., "The Spectrum of Turbulence," *Proceedings of the Royal Society of London*, Vol. A164, 1938, pp 476.

[16] Shinozuka M., and Jan C., "Digital Simulation of Random Processes and Its Applications,"

Journal of Sound and Vibration, Vol. 25, (1), 1972, pp 111-168.

[17] Borgman L.E., "Ocean Wave Simulation for Engineering Design," *Journal of the Waterways and Harbors Division, Proceedings of the American Society of Civil Engineers*, 1969 Vol. 4, pp 557-583.
